Silver-Doped Bioactive Glass/Chitosan Hydrogel with Potential Application in Dental Pulp Repair

Ningxin Zhu,[†] Xanthippi Chatzistavrou,[‡] Petros Papagerakis,[§] Lihong Ge,[†] Man Qin,[†] and Yuanyuan Wang*,[†]

[†]Department of Pediatric Dentistry, School and Hospital of Stomatology, Peking University, #22 Zhongguancun Nandajie, Haidian District, Beijing 100081, China

[‡]Department of Chemical Engineering and Materials Science, Michigan State University, East Lansing, Michigan 48824, United States

[§]College of Dentistry and Biomedical Engineering, Toxicology, Pharmacy/Nutrition, Anatomy and Cell Biology Colleges Graduate Programs, University of Saskatchewan, Saskatoon, Canada

ABSTRACT: The major indications of a successful inflamed-pulp-capping procedure are the formation of a dense calcified dentin barrier and the preservation of healthy pulp tissue concomitant with elimination of inflammation. Our aim is to evaluate the effects of an injectable silver-doped bioactive glass/chitosan hydrogel (Ag-BG/CS), as a pulp-capping material, and explore the molecular mechanisms of Ag-BG/CS in regards to its bioactive and anti-inflammatory properties. First, the structure and component of the material were analyzed by scanning electron microscopy. Then, the downstream molecular mechanisms and anti-inflammatory effects were characterized by quantitative polymerase chain reaction (qPCR) and Western blot. Finally, a preclinical model of rat pulpitis was used to explore the potential of Ag-BG/CS in controlling pulp inflammation *in vivo*. The results showed that Ag-BG/CS induced stronger reparative dentin formation and enhanced preservation of vital pulp tissue when compared to the mineral trioxide aggregate (MTA) which is the currently used clinical standard. Ag-BG/CS also significantly increased the phosphorylation of p38 and ERK1/2(p42/44) of dental pulp cells, indicating that Ag-BG/CS enhanced pulpal repair through the mitogen-activated protein kinase (MAPK) pathway. This novel material may represent a superior solution for dental pulp-capping clinical scenarios with specific advantages for cases of early diffuse pulpitis in immature permanent teeth.

KEYWORDS: silver-doped bioactive glass, chitosan, anti-inflammatory, vital pulp therapy, MAPK pathway, reparative dentin
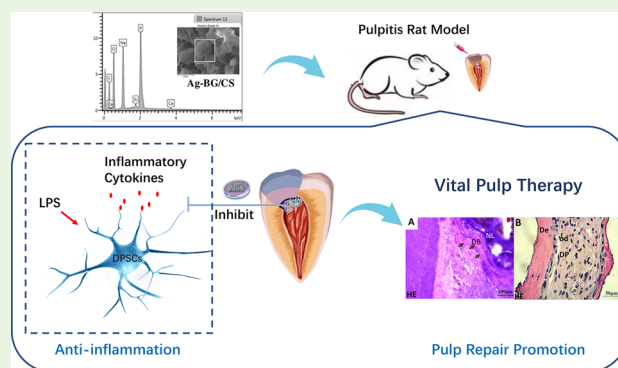
INTRODUCTION

Dental pulp vitality, which is often negatively affected by trauma, morphological abnormalities, or the progression of caries into the pulp chamber, is essential for completion of root development in immature permanent teeth and for maintenance of reparative dentin potential as a response to external stimulation. Accordingly, the conservation of living pulp tissue is essential for successful dental treatment outcomes. Vital pulp therapy (VPT) includes, but is not limited to, direct pulp capping, indirect pulp capping, and partial or full pulpotomy.[1] The key to successful VPT is preservation of the healthy tissue underneath the infection site while treating and regenerating the damaged infected pulp. In a direct pulp-capping procedure, a protective agent is applied to an exposed pulp chamber with the intention of allowing the dental pulp to self-cure and maintaining its normal vitality and function.[2] The only difference between pulpotomy and pulp capping is that, during the pulpotomy, the coronal pulp is wiped away before the capping material is applied.[3] However, pulpotomy is often the preferred course of action owing to the lack of reliable pulp-capping materials with the requisite anti-inflammatory and bioactive properties that help guarantee clinically predictable success.

The most commonly used pulp-capping materials are calcium hydroxide and mineral trioxide aggregate (MTA), both of which have been shown to form well-organized calcified bridges at pulp exposure sites in experimental models.[4−8] MTA is currently considered to be the material of choice for vital pulp-capping treatment, based on studies on its biocompatibility, sealing properties, and ability of inducing mineralized tissue formation. However, most of the studies on MTA use mechanical pulp exposure models in which no

chronic inflammation of the pulp tissue exists.[5,9−11] In fact, for treatment in chronic diffuse pulpitis, MTA falls short of strong antibacterial and anti-inflammatory properties, leaving the possibility of infection recurrence and subsequent death of the whole pulp tissue.[12] Thus, the ideal pulp-capping material for inflamed and immature pulp remains to be discovered.

Bioactive glass is a bone-bonding calcio silicophosphate glass-ceramic material that was discovered in 1969 and reported in 1971 by Hench et al.,[13] claiming that it could bond to collagen fibril layers in bone tissue.[14] Since then, numerous in vitro and in vivo studies have confirmed its strong bioactivity.[15−17] Beginning in 1985, bioactive glasses have been proposed as ideal materials for a number of clinical applications, including middle-ear repair,[18] frontal sinus obliteration,[19] orbital floor reconstruction,[20] and oral-facial applications.[21,22] In vitro and in vivo studies have confirmed that bioactive glass could induce the differentiation of osteo-/odontoblasts[23] and enhance calcified tissue formation.[24−26] Furthermore, modifications of bioactive glass have been shown to improve biological properties,[27] including the addition of silver particles to bioactive glass which has been reported to enhance its bactericidal capacity.[28−30] In 2012, a sol−gel-derived Ag-doped bioactive glass was fabricated,[31] and its physical and biological properties were evaluated.[25,32−34]

The purpose of this study is to evaluate the effects of Ag-BG/CS in vivo, as a pulp-capping material applied in a preclinical pulpitis model, and make comparisons with the most commonly used material in the dental clinics, i.e., mineral trioxide aggregate (MTA). The potential molecular targets of Ag-BG/CS in inflamed dental pulp cells (iDPSCs) are also explored.

■ MATERIALS AND METHODS

Synthesis of Ag-BG/CS and Structural Characterization. The fabrication of Ag-doped bioactive glass (Ag-BG) nanoparticles was performed as previously reported.[32] An amount of 1 mg of chitosan powder (448877, Sigma, USA) was dissolved in 9 mL of hydrochloric acid (0.1 mol/L) with constant stirring for 2 h as component A; β-sodium glycerophosphate powder (Merck, Germany) was dissolved in distilled water as component B (560 g/L); and then component B was added dropwise into component A in an ice bath and mixed adequately into an injectable chitosan/β-sodium glycerophosphate gel (CS gel).[35] The as-synthesized Ag-BG nanoparticles were then mixed with liquid CS gel at a weight ratio of 1:1. The resultant gel was stored at 4 °C until use.

The surface morphology and element component of the synthesized material were investigated by scanning electron microscopy (SEM) analysis and energy spectrum analysis (JSM 7900F, Japan).

Cell Culture. The Ethics Committee of the Peking University Health Science Center reviewed and approved the collection of human dental pulp stem cells (DPSCs) from 14- to 18-year-old patients undergoing dental extraction as part of orthodontic treatment. DPSCs were isolated from the dental pulp space and then digested in 3 mg/mL of type-I collagenase (Sigma-Aldrich, St. Louis, MO, USA) and 4 mg/mL of Dispase (Sigma-Aldrich, St. Louis, MO, USA) for 1 h at 37 °C. Then, the cell suspensions were separated using a 70 μm strainer (Falcon, BD Biosciences, San Jose, CA, USA). The cell suspensions were incubated in α-modified minimum essential medium (α-MEM, GIBCO/BRL, USA) containing 10% fetal bovine serum (FBS, GIBCO, USA), 100 U/mL of penicillin, and 100 μg/mL of streptomycin at 37 °C under 5% CO_2. DPSCs were identified by our previously published method.[37] DPSCs between the fourth and sixth passage were used for this study.

Quantitative Polymerase Chain Reaction Analysis. Following a previously published method,[36] Escherichia coli lipopolysaccharide

(LPS) (Sigma-Aldrich, St Louis, MO, USA) powder was dissolved in sterile distilled water at 1 μg/mL. According to the previous experiments,[37] it had been confirmed that within 6 h the mRNA level of several inflammatory cytokines in LPS-stimulated DPSCs was upregulated most at 1 h. DPSCs subcultured in six-well plates (2 × 10^4 /well) were treated with 1 μg/mL of Escherichia coli lipopolysaccharide for 1 h to trigger inflammation of the DPSCs, and these cells were termed LPS-induced DPSCs (inflamed dental pulp stem cells, iDPSCs). Ag-BG/CS, Ag-BG, CS, and MTA dilutions were prepared through soaking the material in isovolumetric α-MEM and left to stand for 24 h prior to use. IDPSCs were treated with Ag-BG/CS, CS, or MTA dilutions for 1 and 3 h. Untreated DPSCs were termed as the control group, and the iDPSC group, Ag-BG/CS group (iDPSCs + Ag-BG/CS dilution), Ag-BG group (iDPSCs + Ag-BG dilution), CS group (iDPSCs + CS dilution), and MTA group (iDPSCs+ MTA dilution) were compared with the control group at 1 and 3 h. After extracting the RNA from the treated iDPSCs using TRIzol (Introgen, Carlsbad, CA, USA), 1 μg of total RNA was converted to cDNA with Moloney murine leukemia virus reverse transcriptase (M-MLV RTase, Promega, Madison, WI, USA) in a total volume of 20 μL. Quantitative polymerase chain reaction (qPCR) analysis was performed on a total volume of 20 μL in SYBR Green master mix (Rox, Roche Applied Science, IN, USA), with 0.5 μL of cDNA and 200 nM of the primers. The primers were designed by Primer3 and synthesized (BGI, China), and the sequences were listed in Table 1: glyceraldehyde-3-phosphate dehydrogenase

Table 1. Primers Used for Quantitative PCR

target gene	sequence	product size (bp)
GAPDH	forward: GCAAATTCCATGGCACCGTC	465
	reverse: GGGGTCATTGATGGCAACAATA	
DSPP	forward: TCCTAGCAAGATCAAATGTGTCAGT	152
	reverse: CATGCACCAGGACACCACTT	
BSP	forward: ACCCTGCCAAAAGAATGCAG	281
	reverse: TGCCACTAACATGAGGACGT	
RUNX2	forward: CACTGGCGCTGCAACAAGA	157
	reverse: CATTCCGGAGCTCAGCAGAATAA	
IL-1β	forward: TGCACGATGCACCTGTACGA	298
	reverse: AGGCCCAAGGCCACAGGTAT	
IL-6	forward: ACGAACTCCTTCTCCACAAGC	397
	reverse: CTACATTTGCCGAAGAGCCC	
COX-2	forward: CTGGCGCTCAGCCATACAG	401
	reverse: ACACTCATACATACACCTCGGT	
TNF-α	forward: CAGAGGGAAGAGTTCCCCAG	285
	reverse: CCTCAGCTTGAGGGTTTGCTAC	

(GAPDH), dentin sialophosphoprotein (DSPP), interleukin-1β (IL-1β), interleukin-6 (IL-6), interleukin-8 (IL-8), tumor necrosis factor-α (TNF-α), cyclooxygenase-2 (COX-2), alkaline phosphatase (ALP), osteocalcin (OCN), runt-related transcription factor 2 (RUNX2), and bone sialoprotein (BSP). The following thermal cycling conditions were applied: 50 °C for 2 min, then 95 °C for 10 min, followed by 40 cycles of 94 °C for 15 s and 60 °C for 1 min. The reactions were performed using an ABI PRISM 7500 Sequence Detection System (Applied Biosystems, Foster City, CA, USA). The expression level of inflammatory cytokines was evaluated with the primers listed, and the data were analyzed using PRISM 6 software (one-way ANOVA and LSD comparison test).

Enzyme-Linked Immunosorbent Assay Analysis. DPSCs were seeded in 6-well plates (2 × 10^4 /well, expanded ex vivo) and treated with LPS when 80% confluence had been reached. Compared to the mRNA level, the protein level variation is delayed, and thus the iDPSCs were treated with Ag-BG/CS, Ag-BG, CS, and MTA dilutions for 24 h. The level of inflammatory cytokines (IL-1β, IL-6, and TNF-

α) in the supernatants was measured using an IL-1β ELISA kit (QS40181, Qisong, Beijing, China), IL-6 ELISA kit (QS40049, Qisong, Beijing, China), and TNF-α ELISA kit (QS40122, Qisong, Beijing, China) according to the manufacturer's instructions. Concentrations of cytokines were determined using the luminometer plate reader (Molecular Devices, Menlo Park, CA), and the data were analyzed using PRISM 6 software (one-way ANOVA and LSD comparison test).

Western Blot Analysis. DPSCs were seeded in 6-well plates (2 × 10^4 /well, expanded *ex vivo*) and treated with LPS when 80% confluence had been reached. According to the results of qPCR, the iDPSCs were treated with Ag-BG/CS dilutions, p38 mitogen-activated protein kinase (MAPK) pathway inhibitor SB203580 (S1076, Selleck, China), and ERK1/2 (p44/42) MAPK pathway inhibitor SCH772984 (S7101, Selleck, China) for 15 min, 60 min, and 3 h, and then the cells were lysed in RIPA buffer containing protease and phosphatase inhibitors. Proteins were extracted and then quantified using the BCA Protein Assay (Pierce, USA). Approximately 40 μg of the proteins from each sample was separated on 10% SDS-PAGE gels and transferred to PVDF membranes (Millipore, Bedford, MA, USA) at 100 V for 60 min. The membranes were first incubated in blocking buffer (5% nonfat dry milk in Tris-buffered saline containing 0.05% Tween-20, pH 7.4) for 1 h and then incubated with the following antibodies in 1:1000 dilutions at 4 °C overnight: p38 (10A8, 2308T, Cell Signaling Technology, Danvers, MA, USA), phospho-p38 (D3F9, 4511T, Cell Signaling Technology, Danvers, MA, USA), p44/42 MAPK (137F5, Cell Signaling Technology, Danvers, MA, USA), phospho-p44/42 MAPK (4370T, Cell Signaling Technology, Danvers, MA, USA), and β-actin (D6A8, 8457T, Cell Signaling Technology, Danvers, MA, USA). The membranes were incubated in horseradish peroxidase-conjugated secondary antibody (PV9001, PV9002, ZSJQ, China) for 1 h at room temperature, and the bands were visualized using Fusin Fx (Vilber Lourmat, France).

In Vivo **Pulp/Dentin Formation.** Sixteen 8-week-old Balb/c nude mice (Vital River Laboratory Animal Technology, Beijing) were kept in a specific pathogen-free (SPF) level laboratory and, on the day of the experiment, were divided randomly into two groups. In particular, approximately 1.0 × 10^7 DPSC cells (fourth passage) were cultured with Ag-BG/CS dilution, and as a control, the same density of DPSC cells was cultured in extract-free medium. Hydroxyapatite (HA) powder was used as a scaffold for cell growth considering its porous structure. Both groups of DPSC cells were then cocultured separately with 40 mg of HA powder for 3 h before being implanted into the dorsal surfaces of the nude mice. Each mouse received either the experimental or control group of cells/materials. Thus, in total we analyzed eight different samples from the experimental group and eight different samples from the control group. The specimens were recovered by cutting the composite off the dorsal subcutaneous tissue after 8 weeks and fixed with 10% formalin for 24 h, decalcified in 20% ethylene diamine tetraacetic acid (EDTA), and processed for paraffin embedding. The fixed specimens were divided into 4 μm sections and stained with hematoxylin-eosin (HE) for routine histology and Masson's trichrome staining. The samples were examined using an Olympus BX51 microscope (Olympus, Tokyo, Japan). Dentin formation was quantified using Image J (NIH Image software).

Pulpotomy in Rat Model. Ten 6-week-old Wistar male rats (Vital River Laboratory Animal Technology, Beijing) were kept in an SPF level laboratory. All procedures were performed under general anesthesia induced by intraperitoneal injection of 10% chloral hydrate (Hushi, Shanghai, China). The model of early stage pulpitis was established as described previously.[38] Each rat was immobilized, and its mouth was stretched enough to expose the maxillary first molars. Cavities were prepared using a high-speed turbine tooth drill bur (BR-49, ISO001008) with a terminal diameter of 0.5 mm, and the depth of cavities was 1.0 mm. The pulpal exposures were prepared by stabbing gently with a sterile 40# K file through cavities, and coronal pulpal tissue was wiped off. The bleeding exposures were irrigated with normal saline and then treated with sterile cotton balls soaked in 1 μg/mL of *Escherichia coli* LPS for 15 min.[39] Ag-BG/CS was injected in the cavity of the first molar on the right side to cover pulp exposure.

MTA (Dentsply Endodontics, USA) was used to treat the corresponding cavity on the left side for comparison. The coronal cavity was sealed with Fuji IX glass-ionomer cement (GC, Japan).

After 8 weeks, the rats were sacrificed by intraperitoneal injection of 10% chloral hydrate. The specimens were fixed, decalcified, and embedded as above. Fixed specimens were sectioned into 4 μm sections and stained with HE for routine histology. The specimens were examined using immunohistochemistry for differentiation markers' expression. The primary antibodies used were DSPP (1:200, sc-73632, Santa Cruz, CA, USA), vWF (1:200, ZA0111, ZSJQ, Beijing, China), and Nestin (4760T, Cell Signaling Technology, Danvers, MA, USA). The samples were treated with DAB and counterstained with hematoxylin and then examined using an Olympus BX51 microscope (Olympus, Tokyo, Japan).

Statistical Analysis. Comparison of the newly formed mineralized tissues in the two groups was performed via the Wilcoxon test (PRISM6). Comparison between two groups of positive expression cell numbers was performed using the one-way ANOVA and LSD comparison test (PRISM6). The level of significance was set at $p <$ 0.05.

■ RESULTS

Surface Morphology of Ag-BG/CS. The results of scanning electron microscopy (SEM) and energy spectrum analysis revealed that Ag-BGs were rough-surface polygon particles (Figures 1a, 1b), and CS was porous, with the pore diameters reaching 30−40 μm (Figures 1c, 1d). Ag-BG/CS was porous, and the pore diameters were 10−15 μm (Figures 1e, 1f). Ag-BG, CS, and Ag-BG/CS contain O, P, Na, and C
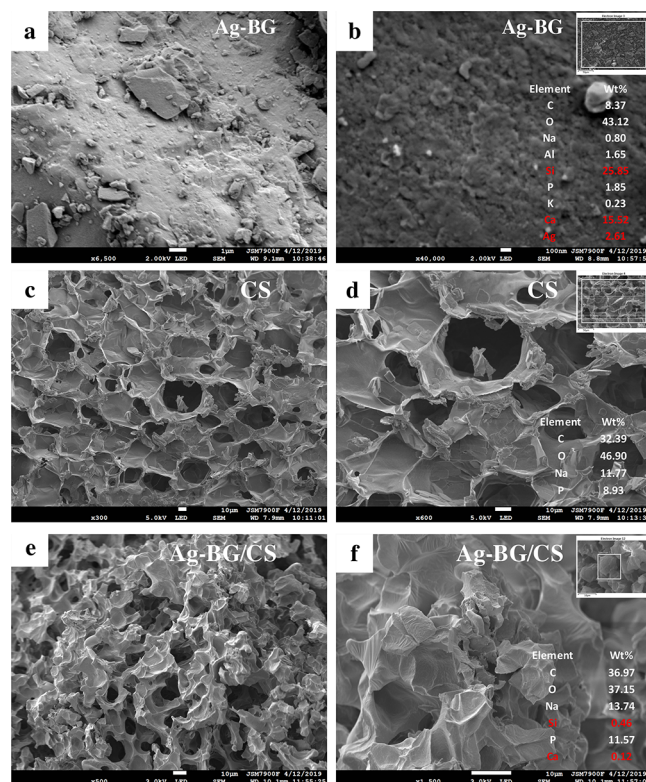

Figure 1. Scanning electron microscopy (SEM) and energy spectrum analysis of Ag-BG, CS, and Ag-BG/CS. Ag-BGs were rough-surface-containing silver, calcium, and silica (a, b). CS was porous, with the pore diameters reaching 30−40 μm, consisting of carbon, oxygen, sodium, and phosphorus (c, d). Ag-BG/CS was porous, and the pore diameters were 10−15 μm. Energy spectrum analysis showed silica and calcium could be examined (e, f).
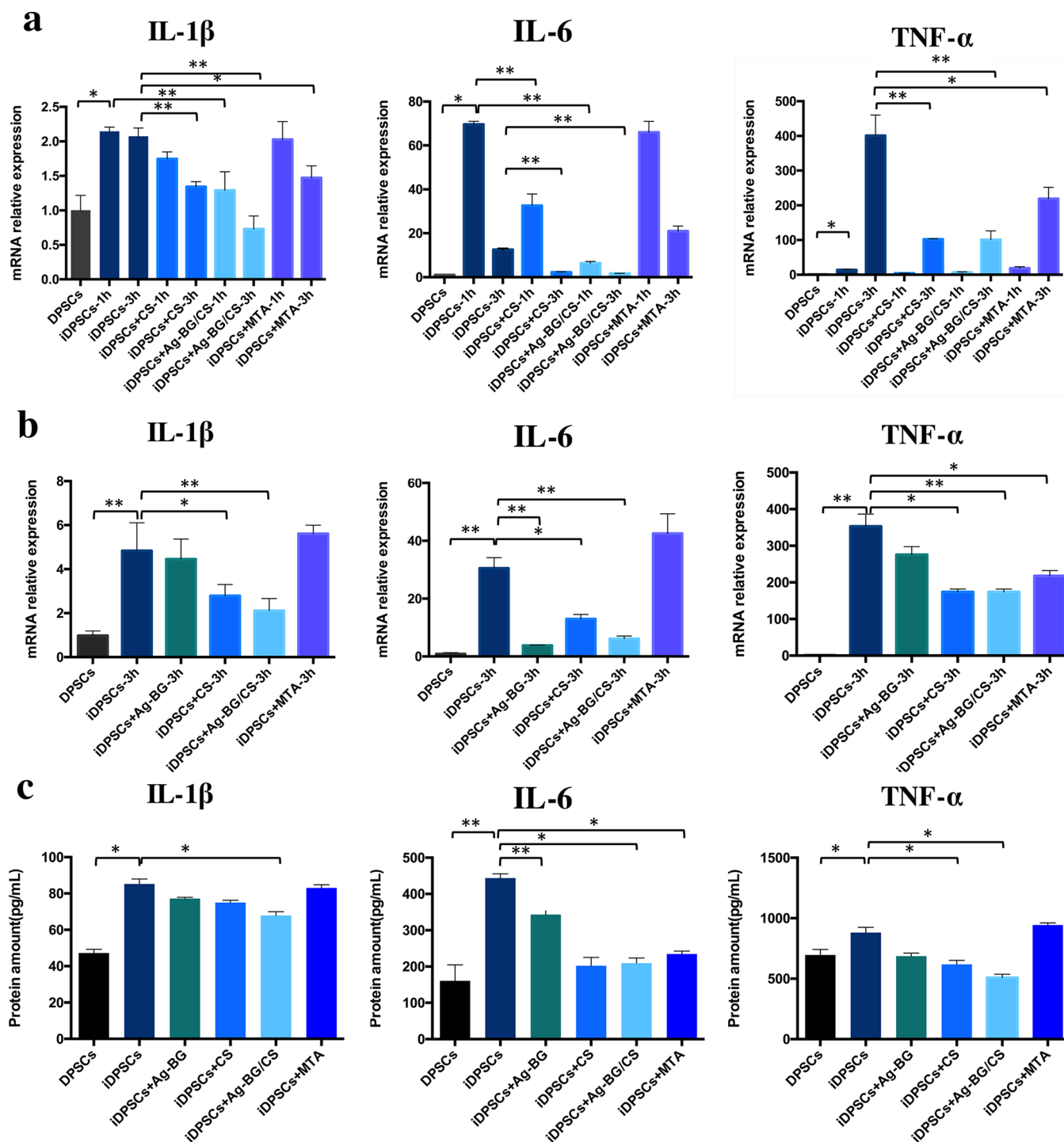
Figure 2. Quantitative PCR (a, b) and ELISA (c) analysis results for the inflammatory cytokines IL-1β, IL-6, and TNF-α upon treatment with Ag-BG/CS, Ag-BG, CS, or MTA. The asterisks indicate significant differences between groups (* $p \leq 0.05$, ** $p \leq 0.01$, *** $p \leq 0.001$, one-way ANOVA and LSD comparison test), and the bars represent the standard deviation of three replicates.

(Figures 1a−1f), whereas Ag-BG contains Ca of 15.52 wt %, Si of 25.85 wt %, Ag of 2.61 wt %, Al of 1.65 wt %, and K of 0.23 wt % (Figure 1b). Although lower than Ag-BG, Si and Ca could also be examined in Ag-BG/CS of 0.46 and 0.12 wt % (Figure 1f), demonstrating Ag-BG was recombined in CS.

Comparison of the Inflammatory Cytokine Profiles of Ag-BG/CS, CS, and MTA. DPSCs were identified in our previously published paper.[37] Quantitative PCR and ELISA analysis were performed, and the results were presented in Figure 2. At 1 and 3 h, the mRNA expression levels of *IL-1β*,

IL-6, and *TNF-α*, which are all known to be involved in dental pulp inflammation, were enhanced by LPS stimulation, as expected. However, Ag-BG/CS significantly downregulated the expression of *IL-1β*, *IL-6*, and *TNF-α* at 3 h, while MTA showed weaker inhibition to these cytokines (Figure 2a). To investigate the anti-inflammatory ability of each component, iDPSCs were treated with Ag-BG, CS, and Ag-BG/CS for 3 h. The expressions of *IL-1β*, *IL-6*, and *TNF-α* were downregulated by Ag-BG and CS, and the complex hydrogel had stronger anti-inflammatory ability (Figure 2b). At the protein
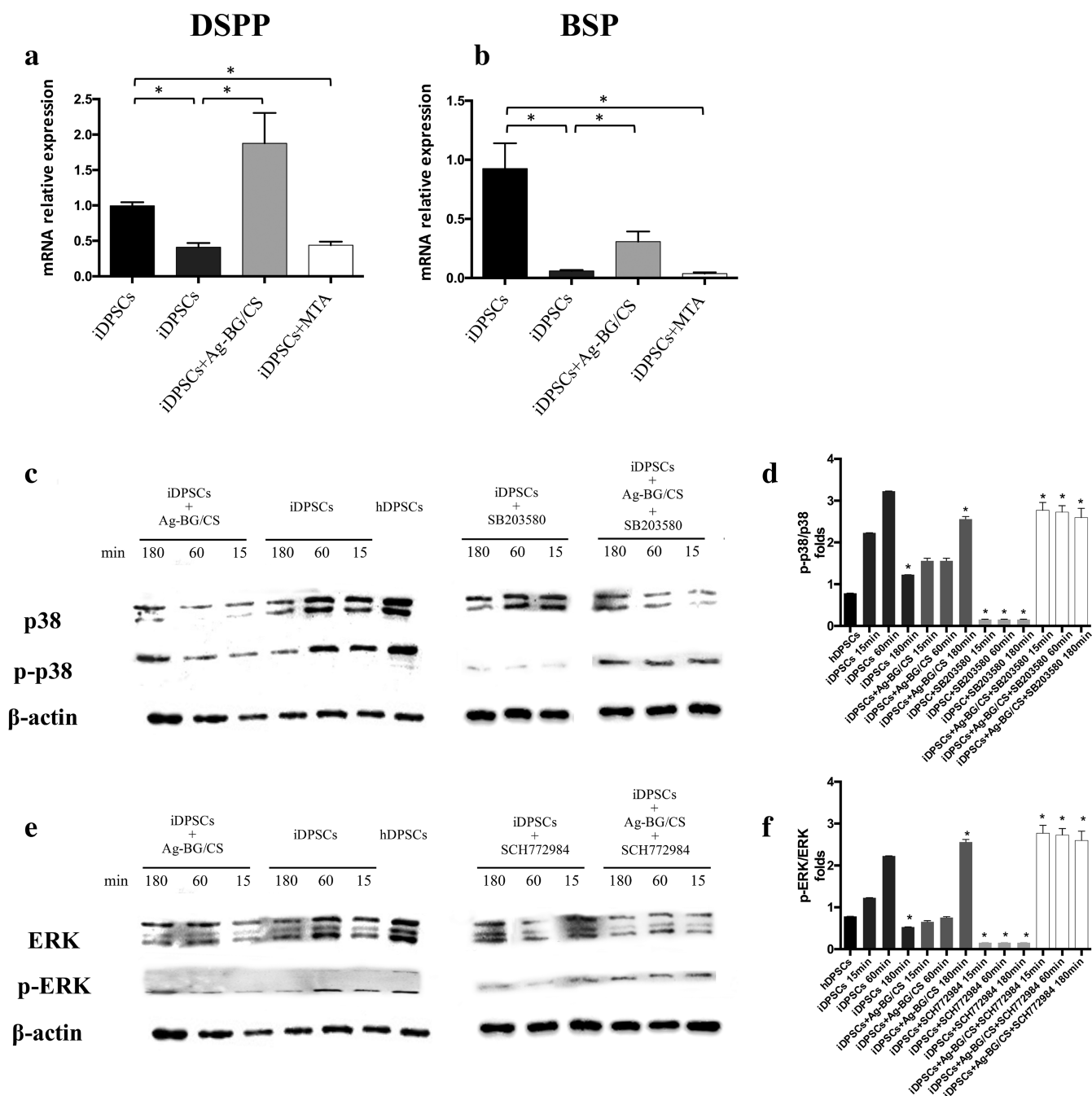
Figure 3. Quantitative PCR and Western blot analysis of the odontoblast differentiation markers BSP and DSPP (a, b) and several important MAPK kinases showing the effects of Ag-BG/CS and MAPK inhibitor SB203580 and SCH772984 (c, e). The asterisks indicate significant differences between groups (* $p \leq 0.05$, ** $p \leq 0.01$, *** $p \leq 0.001$, one-way ANOVA and LSD comparison test), and the bars represent the standard deviation of three replicates.

level, the variation of these inflammatory cytokines was not significant at 3 h (data not shown), but at 24 h, the protein amounts of IL-1β, IL-6, and TNF-α in iDPSCs were significantly suppressed, the same as with the mRNA variation trend (Figure 2c).

Odontogenic Biomarker Expression upon Ag-BG/CS and MTA Treatment. The results of quantitative PCR showed that the mRNA expression of *BSP* and *DSPP*, which are markers of odontoblast differentiation, decreased significantly in the presence of iDPSCs. However, Ag-BG/CS enhanced the expression of *BSP* and *DSPP* in the presence of

iDPSCs, while neither marker showed significant recovery in the MTA group (Figures 3a, 3b).

Activation of the MAPK Pathway through Ag-BG/CS Treatment. In contrast to the control group (DPSC), the amount of phosphorylated p38 and phosphorylated ERK1/2 in the iDPSCs increased significantly upon stimulation by LPS for 15 and 60 min, but in inflamed cells incubated with Ag-BG/CS, the expression levels of both phosphorylated proteins were significantly suppressed within 1 h. Until 3 h, the amount of phosphorylated p38 and phosphorylated ERK1/2 decreased in iDPSCs, and Ag-BG/CS recovered their expression significantly. The classical inhibitor suppressed the expression of
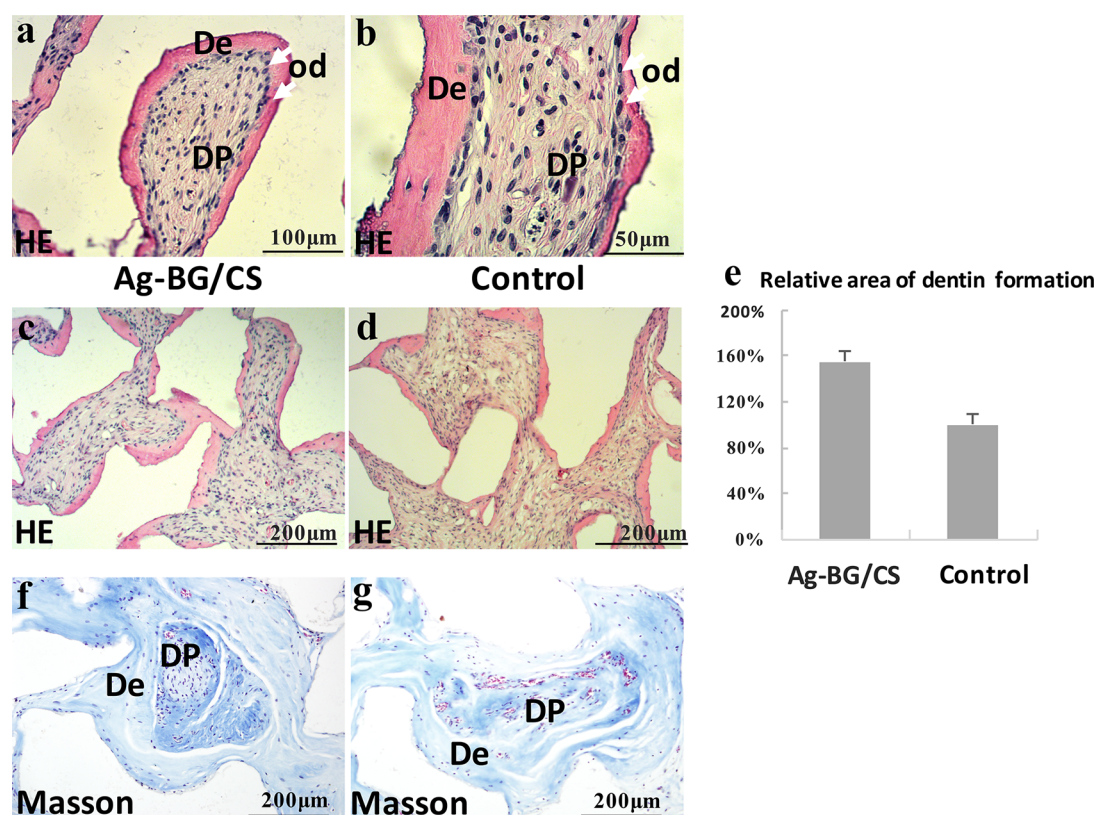
Figure 4. Immunohistochemical staining reagents revealing dentin formation after subcutaneous implantation of DPSCs. HE staining shows the newly formed tissues in both groups (a, b), and the Ag-BG/CS group (c, f) shows higher portion of dentin-like tissue compared to the control group (d, g). Relative areas of dentin formation after treatment with Ag-BG/CS and control group (e). DP refers to dentin/pulp like tissue; De refers to dentin-like tissue: and od refers to odontoblast-like layer.

phosphorylated proteins, and Ag-BG/CS upregulated their expression (Figures 3c, 3e). The relative density of bands was analyzed by ImageJ, and there were significant differences between the iDPSC group and Ag-BG/CS group (Figures 3d, 3f).

In Vivo Formation of the Pulp/Dentin Complex in Nude Mice after DPSC Implantation. After 8 weeks of DPSC implantation, new pulp/dentin complex formation was observed. The implanted DPSCs accumulated and regenerated interstitial tissue (Figures 4a, 4b, DP), and a dentin-like layer (Figures 4a, 4b, De) could also be seen to be interfaced with the dentin/pulp-like fibrous tissue underneath a continuous layer of odontoblast-like cells in both groups (Figures 4a, 4b). The proportion of a dentin-like matrix in the newly formed tissue for the Ag-BG/CS group was higher than that in the control group (Figure 4e). The results of Masson staining showed that the dentin-like layer contained blue-stained collagenous fibers in the Ag-BG/CS group (Figures 4f, De), which is the main component of predentine. However, in the control group, the dentin-like layer (Figure 4g, De) was less than the Ag-BG/CS group.

In Vivo Response to Dental Pulp Capping with MTA and Ag-BG/CS. The _in vivo_ response to Ag-BG/CS was also investigated using a preclinical pulpitis rat model, and the details were given in Table 2. For the LPS-induced inflammatory dental pulp, newly formed dentin-like barriers were observed in both the Ag-BG/CS (Figures 5a, 5b, 5c) and MTA groups (Figures 5d, 5e, 5f) at 8 weeks, and regular fibrous structures could be discerned under higher magnification (Figures 5c, 5f). For the MTA group, most of the

Table 2. Clinical and Histological Assessment of Pulp-Capping Outcomes in a Rat Pulpitis Model

	survival rate	restoration retention	dentin bridge formation	pulp inflammation control yes	no
Ag-BG/CS (n = 10)	9/10	9/9	8/9	7/9	2/9
MTA (n = 10)	9/10	9/9	6/9	4/9	5/9

inflammatory dental pulp tissue was observed to have degenerated (Figure 5d). However, for the Ag-BG/CS group, most of the inflammatory dentin pulp tissue was observed to have maintained its regular structure, as seen in the apical pulp tissue area (Figures 5a).

To study the differentiation potential of the DPSCs after pulp-capping, immunohistochemistry was applied to detect the expression of functional odontoblast biomarkers. In the Ag-BG/CS group, a strong Dspp immunoreactivity was observed in the outer portion of the pulp where odontoblast-like cells could be seen (Figure 5g) together with strong Nestin expression (Figure 5i) and high vWF expression around the tube-like structures near the dentin-like layer (Figure 5h). In contrast, only light immunoreactivity was detected in the degenerated pulp tissue of the MTA group (Figures 5j, 5k, 5l).

■ **DISCUSSION**

Pulp tissue is often affected due to dental caries, developmental defects, or traumatic injuries. When the inflammation is
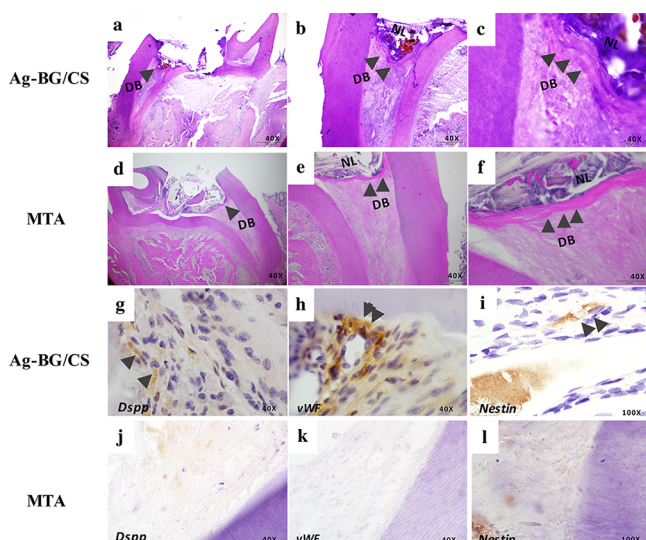
Figure 5. HE staining showing regenerated dentin-like tissue after pulp-capping experiments using Ag-BG/CS (a, b, c) and MTA (d, e, f) and the expression of the odontoblast biomarkers Dspp, vWF, and nestin after using Ag-BG/CS (g, h, i) and MTA (j, k, l).

circumscribed, pulp capping or pulpotomy is applied to preserve the vitality of the apical and/or coronal pulpal tissue, aiming to promote dentin repair and deal with inflammation. However, these approaches are not efficient for the diffused or chronic pulpitis because they cannot deal efficiently against both the chronic inflammation control and the dentin tissue repair. Therefore, there is a clear need for a biocompatible capping material with strong antibacterial and anti-inflammatory properties to treat pulpitis with extensive inflammation to avoid extensive endodontic treatments.[40] Bioactive glass and bioceramics have confirmed osteoconductive properties *in vitro* and *in vivo*,[24,26,41,42] and they are able to induce calcified barrier formation in pulp exposure models,[43] preserving the remaining uninfected dental pulp cells. It has also been reported that, in the presence of critical concentrations of silicon and calcium ions, the alkaline phosphatase activities of the pulp cells are enhanced, and osteoblasts are able to begin to proliferate and regenerate new bone and to differentiate into mature osteocyte phenotypes within 48 h.[15,44] In previous research, the concentration of calcium ions released from a Ag-doped bioactive glass sol−gel after soaking in Tris buffer for 100 h exceeded 40 ppm, while that of silicon ions reached 30 ppm. Ag-doped BG has a slightly higher negative value compared to Ag-free BG, which might indicate enhanced bioactive behavior.[33] In the current study, DPSCs pretreated with a Ag-BG/CS dilution produced a more dentin-like matrix when implanted subcutaneously compared to that produced by untreated DPSCs, indicating that Ag-BG/CS strongly induces the odontogenic potential of DPSCs *in vivo*.

When dental pulp is affected by carious lesions or mechanical trauma, the vital tissues become inflamed. Low-grade inflammation may trigger regenerative mechanisms, including angiogenic and stem cell processes,[45] and tertiary dentine is deposited in response to relatively intense stimulus by secretion from the new generation of odontoblast-like cells that have become differentiated from the stem/progenitor cell populations.[45] It has been reported that, in the early stage of inflammation, the locally derived growth factors, neuro-peptides, and cytokines are released from the host dentine

matrix and by resident pulpal cells, immune cells, neurons, and/or dying cells and modulate the defense and repair processes within the tissue.[45] Chitosan has revolutionized various areas of medicine, food, agriculture, and environmentalism owing to its biocompatibility, biodegradability, nontoxicity, plasticity,[46] and high drug-loading capacity.[47] *In vitro* experiments have demonstrated that inflammatory cytokines in fibroblasts are suppressed in media supplemented with CS monomers, and that infiltrating inflammation is eliminated by capping with CS *in vivo*.[48] In dental pulp exposure dog models, treatment using a CS bilayer membrane bearing microspheres containing TGF-β1 led to the generation of much more reparative dentin *in vivo* compared to that generated using Dycal.[49] It has also been reported that DPSCs grow well in CS/β-glycerophosphate/hydroxyapatite (CS/GP/HA) hydrogel, and the ALPase enzymatic activity of DPSCs was enhanced in both CS/GP and CS/GP/HA hydrogels.[50] In the current study, thermosensitive CS/GP hydrogel was chosen as the injectable delivery vehicle owing to its favorable operability and slow biodegradation, which permits the controlled and sustained release of loaded moieties.[47] According to the data presented here, Ag-BG and CS alone suppressed the expression of inflammatory cytokines, and Ag-BG/CS downregulated the expression level further, confirming its superior anti-inflammatory properties. The results suggest that, in our model, Ag-BG and CS both contribute to the anti-inflammatory activity of Ag-BG/CS.

The early formation of dentin bridges is a convincing indicator for the recovery of damaged pulp tissue.[40] However, under severe inflammation conditions such as chronic or diffuse pulpitis, most of the cells are inflamed, which can rapidly result in necrosis of the pulpal tissue. Therefore, in such scenarios, there is a clear need for a biocompatible capping material with strong antibacterial and anti-inflammatory properties for the treatment of severe pulpitis and the avoidance of extensive endodontic treatments, and various kinds of pulp-capping materials have been tested in numerous studies, including several bioactive materials. A mineral trioxide aggregate (MTA) was introduced by Torabinejad in the early 1900s.[51] Since then, MTA, a common capping material, has been widely studied, and these studies confirmed its ability to form a more predictable hard tissue barrier in comparison to calcium hydroxide[5,8] and other materials, while causing similar or slightly less pulpal inflammation. It has been also consistently acknowledged that MTA has favorable mineralized-inducing ability in pulpotomy models performed in healthy teeth after accidental pulp tissue exposure.[52] However, only few reports exist on MTA application on inflammatory pulp tissue. In our studies using a pulpitis rat model, the inflammatory status of the tissue was well controlled by Ag-BG/CS capping treatment, which resulted in a newly formed calcified barrier beneath the exposure location at 8 weeks together with well-organized pulpal tissue at the apical end. In addition, the positive expression of the odontogenic and angiogenic factors was strongly detected in the Ag-BG/CS group but not in the MTA group, suggesting that the better cellular response to inflammation seen in the Ag-BG/CS group was due to molecular changes of the expression levels of key players for tissue regeneration and repair.

vWF, called at the time FVIII-related antigen, is a large glycoprotein which mediates platelet adhesion to the subendothelium following vascular injury and stabilizes coagulation Factor VIII,[53] often used as a marker for

endothelial cells.[54,55] In the current study, vWF-marked vessel-like structures were observed for the Ag-BG/CS group, but the expression of vWF was minimal in the MTA-treated group. Furthermore, dentin sialophosphoprotein (Dspp), a phosphorylated protein that is a major component of non-collagenous dentin extracellular matrices mainly expressed in odontoblasts,[56] was more strongly expressed contiguous to predentine under Ag-BG/CS treatment than that in the MTA-treated group. Additionally, nestin, a common marker of neural stem cells, was also more strongly expressed in the Ag-BG/CS group than in the MTA group. All the above suggest that Ag-BG/CS has superior properties compared to MTA in terms of dentin and endothelium biomarker expression.

On the other hand, in the Ag-BG/CS group, the pulp tissue degenerated to fibrosis in the coronal canal, while the apical tissue maintained its vital structure, indicating that Ag-BG/CS is able to reduce inflammation, resulting in the preservation of the resident pulp tissue in the apical root and therefore its essential functionality and vitality. In contrast, a well-organized dentin-like barrier could be observed in MTA-treated teeth due to its good odontoblastic inducibility; however, the apical pulp tissue showed persistent inflammation, and these markers were barely expressed in the affected tissue, indicating that the residual pulp tissue failed to recover from its inflamed condition with MTA treatment due to its poor anti-inflammatory activity. Thus, the results suggest that Ag-BG/CS is better than MTA for treating dental pulp inflammation.

It had been reported that NF-κB and MAPK signaling pathways played an important role in osteoclast differentiation,[57] and the NF-κB pathway was associated with inflammation led by LPS in DPSCs.[58,59] In our previous study, this material had been shown to inhibit the phosphorylation of p65 at the protein level and the nuclear accumulation of p65 in DPSCs.[37] Thus, we hypothesized that NF-κB signaling plays a crucial role in the effects of Ag-BG/CS on inflamed DPSCs. An important upstream component of the NF-κB pathway is MAPK proteins, which are essential components of the signal transduction system and comprise three clearly characterized families: extracellular signal regulated kinases (ERKs), c-Jun N-terminal kinases (JNKs), and p38 MAPKs.[60] MAPK signaling plays a critical role in stem cell differentiation,[61] and they have been implicated as key regulators of pro-inflammatory cytokine (such as IL-6 and TNF) production.[62,63] Among these kinases, p38 MAPK has been reported to be involved in odontoblast stimulation during tertiary dentinogenesis,[64] as well as a modulator of the NF-κB pathway,[65] and its activity is critical for normal immune and inflammatory responses. ERK1/2 signaling has been implicated as a key regulator of cell proliferation and differentiation.[61] It had been reported that LPS could induce inflammatory cytokine release by enhancing the phosphorylation of p38, ERK, and JNK MAPKs,[62] and inflammation in dental pulpitis could be suppressed through blocking the MAPK pathway.[66] A previous study implied that MTA could activate the MAPK pathway during repair response of the dentin–pulp complex.[67] In our research, Ag-BG/CS dilutions increased the phosphorylation of p38 and ERK1/2, indicating that Ag-BG/CS induces pulp repair via activation of the ERK1/2 MAPK pathway. Ag-BG/CS significantly downregulated all the inflammatory markers studied here, most likely through modulation of the p38 MAPKs signaling pathway.

The mechanism might result from the richness of calcium in both Ag-BG/CS and MTA, which could activate the Ca^{2+}/ calmodulin-dependent kinase II (CaMK II). It had been demonstrated that CaMK II was associated with osteo-/ odontogenic differentiation,[68] and its activation could elicit the phosphorylation of p38, ERK1/2, and JNK MAPK cascades.[69,70] The differences between Ag-BG/CS and MTA might be due to the amount of bioactive components such as calcium ions and chitosan. Thus, our results support the hypothesis that infected pulpal cells could recover from inflammation under Ag-BG/CS treatment through the MAPK pathway, maintaining their ability to self-cure. However, inflamed tissue in the MTA group degenerates to eventual necrosis due to its poor anti-inflammatory properties, resulting in diminished reparative dentine formation.

■ CONCLUSIONS

In the present research, Ag-BG/CS has been proven to downregulate the inflammatory cytokines and to induce inflamed pulp cells to form mineralized barriers in vitro and in vivo. The data also indicate that this novel material promotes pulpal self-curing, possibly through the activation of the MAPK pathway. Thus, Ag-BG/CS exhibits multiple bioactive properties and represents a potential pulp-capping agent for the early treatment of diffuse pulpitis. Ag-BG/CS promotes affected tissue recovery and increases the pulp tissue retention rate of pulp-affected immature permanent teeth. Further preclinical studies and well-designed clinical trials may provide recommendations for clinical use of Ag-BG/CS in cases of chronic diffuse pulpitis.

■ AUTHOR INFORMATION

Corresponding Author

*E-mail: cwyyd@126.com. Tel.: 8610 82195306. Fax: 8610 82195361.

Notes

The authors declare no competing financial interest.

■ ACKNOWLEDGMENTS

■ REFERENCES

(1) Miyashita, H.; Worthington, H. V.; Qualtrough, A.; Plasschaert, A. WITHDRAWN: Pulp management for caries in adults: maintaining pulp vitality. Cochrane Database Syst. Rev. 2016, 11, CD004484.

(2) Miyashita, H.; Worthington, H. V.; Qualtrough, A.; Plasschaert, A. Pulp management for caries in adults: maintaining pulp vitality. Cochrane Database Syst. Rev. 2007, No. 2, CD004484.

(3) Gandolfi, M. G.; Spagnuolo, G.; Siboni, F.; Procino, A.; Rivieccio, V.; Pelliccioni, G. A.; Prati, C.; Rengo, S. Calcium silicate/calcium phosphate biphasic cements for vital pulp therapy: chemical-physical properties and human pulp cells response. Clin Oral Investig 2015, 19 (8), 2075–89.

(4) Schröder, U. Effects of calcium hydroxide-containing pulp-capping agents on pulp cell migration, proliferation, and differentiation. J. Dent. Res. 1985, 64 (4), 541–548.

(5) Aeinehchi, M.; Eslami, B.; Ghanbariha, M.; Saffar, A. Mineral trioxide aggregate (MTA) and calcium hydroxide as pulp-capping agents in human teeth: a preliminary report. International Endodontic Journal 2003, 36 (3), 225–235.

(6) Lu, Y.; Liu, T.; Li, H.; Pi, G. Histological evaluation of direct pulp capping with a self-etching adhesive and calcium hydroxide on human pulp tissue. Int. Endod J. 2008, 41 (8), 643–50.

(7) Garrocho-Rangel, A.; Flores, H.; Silva-Herzog, D.; Hernandez-Sierra, F.; Mandeville, P.; Pozos-Guillen, A. J. Efficacy of EMD versus calcium hydroxide in direct pulp capping of primary molars: a randomized controlled clinical trial. *Oral Surg Oral Med. Oral Pathol Oral Radiol Endod* **2009**, *107* (5), 733–8.

(8) Abedi, H. R.; Torabinejad, M.; Pitt Ford, T. R. The use of mineral trioxide aggregate cement (MTA) as a direct pulp-capping agent. **1996**; Vol. 22.

(9) Salako, N.; Joseph, B.; Ritwik, P.; Salonen, J.; John, P.; Junaid, T. A. Comparison of bioactive glass, mineral trioxide aggregate, ferric sulfate, and formocresol as pulpotomy agents in rat molar. *Dent. Traumatol.* **2003**, *19* (6), 314–320.

(10) Farsi, N.; Alamoudi, N.; Balto, K.; Al, M. Clinical Assessment of Mineral Trioxide Aggregate (MTA) as Direct Pulp Capping in Young Permanent Teeth. *Journal of Clinical Pediatric Dentistry* **2007**, *31* (2), 72–76.

(11) Tuna, D.; Olmez, A. Clinical long-term evaluation of MTA as a direct pulp capping material in primary teeth. *Int. Endod J.* **2008**, *41* (4), 273–8.

(12) Kim, D.-H.; Jang, J.-H.; Lee, B.-N.; Chang, H.-S.; Hwang, I.-N.; Oh, W.-M.; Kim, S.-H.; Min, K.-S.; Koh, J.-T.; Hwang, Y.-C. Anti-inflammatory and Mineralization Effects of Pro Root MTA and Endocem MTA in Studies of Human and Rat Dental Pulps In Vitro and In Vivo. *J. Endodont* **2018**, *44* (10), 1534–1541.

(13) Hench, L. L.; Splinter, R. J.; Allen, W. C.; Greenlee, T. K. *J. Biomed. Mater. Res.* **1971**, *5*, 117–141.

(14) Hench, L. L.; Clark, A. E.; Schaake, H. F. Effects of microstructure on the radiation stability of amorphous semi-conductors. *J. Non-Cryst. Solids* **1972**, *8–10*, 837–843.

(15) Hench, L.; Hench, J.; Greenspan, D. Bioglass: a short history and bibliography. *J. Australian Ceramic Soc.* **2004**, *40* (1), 1.

(16) Nakamura, T.; Yamamuro, T.; Higashi, S.; Kokubo, T.; Itoo, S. A new glass-ceramic for bone replacement: Evaluation of its bonding to bone tissue. *J. Biomed. Mater. Res.* **1985**, *19* (6), 685–698.

(17) Clupper, D.; Hench, L. Bioactive response of Ag-doped tape cast Bioglass 45S5 following heat treatment. *J. Mater. Sci.: Mater. Med.* **2001**, *12* (12), 917–921.

(18) Merwin, G. E. Bioglass Middle Ear Prosthesis: Preliminary Report. *Ann. Otol., Rhinol., Laryngol.* **1986**, *95* (1), 78–82.

(19) Peltola, M.; Suonpää, J.; Määttänen, H.; Varpula, M.; Aitasalo, K. Clinical follow-up method for frontal sinus obliteration with bioactive glass S53P4. *J. Biomed. Mater. Res.* **2001**, *58* (1), 54.

(20) Aitasalo, K.; Kinnunen, I.; Palmgren, J.; Varpula, M. Repair of orbital floor fractures with bioactive glass implants. *Journal of Oral & Maxillofacial Surgery Official Journal of the American Association of Oral & Maxillofacial Surgeons* **2001**, *59* (12), 1390–1395.

(21) Stanley, H. R.; Clark, A. E.; Pameijer, C. H.; Louw, N. P. Pulp capping with a modified bioglass formula (#A68-modified). *Am. J. Dentistry* **2001**, *14* (4), 227–232.

(22) Gillam, D. G.; Tang, J. Y.; Mordan, N. J.; Newman, H. N. The effects of a novel Bioglass dentifrice on dentine sensitivity: a scanning electron microscopy investigation. *J. Oral Rehabil.* **2002**, *29* (4), 305–313.

(23) Hench, L. The story of Bioglass. *J. Mater. Sci.: Mater. Med.* **2006**, *17* (11), 967–978.

(24) Meretoja, V. V.; Tirri, T.; Malin, M.; Seppala, J. V.; Narhi, T. O. Ectopic bone formation in and soft-tissue response to P(CL/DLLA)/bioactive glass composite scaffolds. *Clin Oral Implants Res.* **2014**, *25* (2), 159–64.

(25) Wang, Y.; Chatzistavrou, X.; Faulk, D.; Badylak, S.; Zheng, L.; Papagerakis, S.; Ge, L.; Liu, H.; Papagerakis, P. Biological and bactericidal properties of Ag-doped bioactive glass in a natural extracellular matrix hydrogel with potential application in dentistry. *European Cells & Materials* **2015**, *29*, 342–355.

(26) Nommeots-Nomm, A.; Labbaf, S.; Devlin, A.; Todd, N.; Geng, H.; Solanki, A. K.; Tang, H. M.; Perdika, P.; Pinna, A.; Ejeian, F.; Tsigkou, O.; Lee, P. D.; Esfahani, M. H. N.; Mitchell, C. A.; Jones, J. R. Highly degradable porous melt-derived bioactive glass foam scaffolds for bone regeneration. *Acta Biomater.* **2017**, *57*, 449–461.

(27) Abe, Y.; Kokubo, T.; Yamamuro, T. Apatite coating on ceramics, metals and polymers utilizing a biological process. *J. Mater. Sci.: Mater. Med.* **1990**, *1* (4), 233–238.

(28) Wren, A. W.; Hassanzadeh, P.; Placek, L. M.; Keenan, T. J.; Coughlan, A.; Boutelle, L. R.; Towler, M. R. Silver Nanoparticle Coated Bioactive Glasses–Composites with Dex/CMC Hydrogels: Characterization, Solubility, and In Vitro Biological Studies. *Macromol. Biosci.* **2015**, *15* (8), 1146–58.

(29) Shih, S. J.; Tzeng, W. L.; Jatnika, R.; Shih, C. J.; Borisenko, K. B. Control of Ag nanoparticle distribution influencing bioactive and antibacterial properties of Ag-doped mesoporous bioactive glass particles prepared by spray pyrolysis. *J. Biomed. Mater. Res., Part B* **2015**, *103* (4), 899–907.

(30) Gholipourmalekabadi, M.; Nezafati, N.; Hajibaki, L.; Mozafari, M.; Moztarzadeh, F.; Hesaraki, S.; Samadikuchaksaraei, A. Detection and qualification of optimum antibacterial and cytotoxic activities of silver-doped bioactive glasses. *IET Nanobiotechnol.* **2015**, *9* (4), 209–14.

(31) Chatzistavrou, X.; Kontonasaki, E.; Bakopoulou, A.; Theocharidou, A.; Sivropoulou, A.; Paraskevopoulos, K. M.; Koidis, P.; Boccaccini, A. R.; Kasuga, T. Development of new sol-gel derived Ag-doped biomaterials for dental applications. *MRS Proceedings* **2012**, DOI: 10.1557/opl.2012.743.

(32) Chatzistavrou, X.; Tsigkou, O.; Amin, H. D.; Paraskevopoulos, K. M.; Salih, V.; Boccaccini, A. R. Sol-gel based fabrication and characterization of new bioactive glass-ceramic composites for dental applications. *J. Eur. Ceram. Soc.* **2012**, *32* (12), 3051–3061.

(33) Chatzistavrou, X.; Fenno, J. C.; Faulk, D.; Badylak, S.; Kasuga, T.; Boccaccini, A. R.; Papagerakis, P. Fabrication and characterization of bioactive and antibacterial composites for dental applications. *Acta Biomater.* **2014**, *10* (8), 3723–32.

(34) Chatzistavrou, X.; Velamakanni, S.; DiRenzo, K.; Lefkelidou, A.; Fenno, J. C.; Kasuga, T.; Boccaccini, A. R.; Papagerakis, P. Designing dental composites with bioactive and bactericidal properties. *Mater. Sci. Eng., C* **2015**, *52*, 267–272.

(35) Supper, S.; Anton, N.; Seidel, N.; Riemenschnitter, M.; Curdy, C.; Vandamme, T. Thermosensitive chitosan/glycerophosphate-based hydrogel and its derivatives in pharmaceutical and biomedical applications. *Expert Opin. Drug Delivery* **2014**, *11* (2), 249–67.

(36) He, W.; Wang, Z.; Luo, Z.; Yu, Q.; Jiang, Y.; Zhang, Y.; Zhou, Z.; Smith, A. J.; Cooper, P. R. LPS promote the odontoblastic differentiation of human dental pulp stem cells via MAPK signaling pathway. *J. Cell. Physiol.* **2015**, *230* (3), 554–61.

(37) Zhu, N.; Chatzistavrou, X.; Ge, L.; Qin, M.; Papagerakis, P.; Wang, Y. Biological properties of modified bioactive glass on dental pulp cells. *J. Dent.* **2019**, *83*, 18–26.

(38) Watts, A.; Paterson, R. C. Bacterial contamination as a factor influencing the toxicity of materials to the exposed dental pulp. *Oral Surg., Oral Med., Oral Pathol.* **1987**, *64* (4), 466–474.

(39) Tao, Y. U.; J, T.; Qing-Mei, W. E. I; Yi-Fen, L. I; Kaplan, D. L. Wound healing effects of silk fibroin-bone morphogenetic protein-2 scaffolds on inflammatory pulp in rats. *J. Peking University (Health Sciences)* **2015**, *47* (5), 814–819.

(40) Goldberg, M.; Smith, A. J. Cells and Extracellular Matrices of Dentin and Pulp: A Biological Basis for Repair and Tissue Engineering. *Crit. Rev. Oral Biol. Med.* **2004**, *15* (1), 13–27.

(41) Shrestha, S.; Kishen, A. Bioactive Molecule Delivery Systems for Dentin-pulp Tissue Engineering. *J. Endod* **2017**, *43* (5), 733–744.

(42) Gala-Garcia, A.; Teixeira, K.; Wykrota, F.; Sinisterra, R.; Cortés, M. Bioceramic/poly (glycolic)-poly (lactic acid) composite induces mineralized barrier after direct capping of rat tooth pulp tissue. *Brazilian Oral Research* **2010**, *24* (1), 8.

(43) Gala-Garcia, A.; Teixeira, K. I.; Wykrota, F. H.; Sinisterra, R. D.; Cortes, M. E. Bioceramic/poly (glycolic)-poly (lactic acid) composite induces mineralized barrier after direct capping of rat tooth pulp tissue. *Braz Oral Res.* **2010**, *24* (1), 8–14.

(44) Xynos, I. D.; Edgar, A. J.; Buttery, L. D.; Hench, L. L.; Polak, J. M. Ionic products of bioactive glass dissolution increase proliferation of human osteoblasts and induce insulin-like growth factor II mRNA

expression and protein synthesis. *Biochem. Biophys. Res. Commun.* **2000**, *276* (2), 461−465.

(45) Cooper, P. R.; Takahashi, Y.; Graham, L. W.; Simon, S.; Imazato, S.; Smith, A. J. Inflammation-regeneration interplay in the dentine-pulp complex. *J. Dent.* **2010**, *38* (9), 687−97.

(46) Rani, M.; Agarwal, A.; Negi, Y. S. Review: Chitosan based hydrogel polymeric beads - As drug delivery system. *BioResources* **2010**, 2865.

(47) Rajitha, P.; Gopinath, D.; Biswas, R.; Sabitha, M.; Jayakumar, R. Chitosan nanoparticles in drug therapy of infectious and inflammatory diseases. *Expert Opin. Drug Delivery* **2016**, *13* (8), 1177−94.

(48) Matsunaga, T.; Yanagiguchi, K.; Yamada, S.; Ohara, N.; Ikeda, T.; Hayashi, Y. Chitosan monomer promotes tissue regeneration on dental pulp wounds. *J. Biomed. Mater. Res., Part A* **2006**, *76* (4), 711−20.

(49) Li, F.; Liu, X.; Zhao, S.; Wu, H.; Xu, H. H. Porous chitosan bilayer membrane containing TGF-beta1 loaded microspheres for pulp capping and reparative dentin formation in a dog model. *Dent. Mater.* **2014**, *30* (2), 172−81.

(50) Chen, Y.; Zhang, F.; Fu, Q.; Liu, Y.; Wang, Z.; Qi, N. In vitro proliferation and osteogenic differentiation of human dental pulp stem cells in injectable thermo-sensitive chitosan/beta-glycerophosphate/hydroxyapatite hydrogel. *J. Biomater. Appl.* **2016**, *31* (3), 317−27.

(51) Abedi, H. R.; et al. OR 44 The use of mineral tri-oxide aggregate cement (MTA) as a direct pulp capping agent. *J. Endodont* **1996**, *22* (4), 199.

(52) Ohkura, N.; Edanami, N.; Takeuchi, R.; Tohma, A.; Ohkura, M.; Yoshiba, N.; Yoshiba, K.; Ida-Yonemochi, H.; Ohshima, H.; Okiji, T.; Noiri, Y. Effects of pulpotomy using mineral trioxide aggregate on prostaglandin transporter and receptors in rat molars. *Sci. Rep.* **2017**, *7* (1), 6870.

(53) Randi, A. M.; Smith, K. E.; Castaman, G. Von Willebrand factor regulation of blood vessel formation. *Blood* **2018**, *132*, 132.

(54) Denis, C. V.; Lenting, P. J. von Willebrand factor: at the crossroads of bleeding and thrombosis. *Int. J. Hematol.* **2012**, *95* (4), 353−61.

(55) Xiang, Y.; Hwa, J. Regulation of VWF expression, and secretion in health and disease. *Curr. Opin. Hematol.* **2016**, *23* (3), 288−293.

(56) Chen, S.; Gluhak-Heinrich, J.; Wang, Y. H.; Wu, Y. M.; Chuang, H. H.; Chen, L.; Yuan, G. H.; Dong, J.; Gay, I.; MacDougall, M. Runx2, osx, and dspp in tooth development. *J. Dent. Res.* **2009**, *88* (10), 904−909.

(57) Wada, T.; Nakashima, T.; Hiroshi, N.; Penninger, J. M. RANKL-RANK signaling in osteoclastogenesis and bone disease. *Trends Mol. Med.* **2006**, *12* (1), 17−25.

(58) Feng, G.; Zheng, K.; Cao, T.; Zhang, J.; Lian, M.; Huang, D.; Wei, C.; Gu, Z.; Feng, X. Repeated stimulation by LPS promotes the senescence of DPSCs via TLR4/MyD88-NF-κB-p53/p21 signaling. *Cytotechnology* **2018**, *70* (3), 1023−1035.

(59) Yuan, H.; Zhang, H.; Hong, L.; Zhao, H.; Wang, J.; Li, H.; Che, H.; Zhang, Z. MicroRNA let-7c-5p Suppressed Lipopolysaccharide-Induced Dental Pulp Inflammation by Inhibiting Dentin Matrix Protein-1-Mediated Nuclear Factor kappa B (NF-κB) Pathway In Vitro and In Vivo. *Med. Sci. Monit.* **2018**, *24*, 6656−6665.

(60) McGrath, M. A.; Harnett, M. M.; Thalhamer, T. MAPKs and their relevance to arthritis and inflammation. *Rheumatology* **2007**, *47* (4), 409−414.

(61) Roux, P. P.; Blenis, J. ERK and p38 MAPK-activated protein kinases: a family of protein kinases with diverse biological functions. *Microbiol Mol. Biol. Rev.* **2004**, *68* (2), 320−344.

(62) Hu, T.-Y.; Ju, J.-M.; Mo, L.-H.; Ma, L.; Hu, W.-H.; You, R.-R.; Chen, X.-Q.; Chen, Y.-Y.; Liu, Z.-Q.; Qiu, S.-Q.; Fan, J.-T.; Cheng, B.-H. Anti-inflammation action of xanthones from Swertia chirayita by regulating COX-2/NF-κB/MAPKs/Akt signaling pathways in RAW 264.7 macrophage cells. *Phytomedicine* **2019**, *55*, 214−221.

(63) Darling, N. J.; Cook, S. J. The role of MAPK signalling pathways in the response to endoplasmic reticulum stress. *Biochim. Biophys. Acta, Mol. Cell Res.* **2014**, *1843* (10), 2150−2163.

(64) Simon, S.; Smith, A. J.; Berdal, A.; Lumley, P. J.; Cooper, P. R. The MAP kinase pathway is involved in odontoblast stimulation via p38 phosphorylation. *J. Endod* **2010**, *36* (2), 256−9.

(65) Hoesel, B.; Schmid, J. A. The complexity of NF-κB signaling in inflammation and cancer. *Mol. Cancer* **2013**, *12* (1), 86.

(66) Mahmoud Hashemi, A.; Solahaye Kahnamouii, S.; Aghajani, H.; Frozannia, K.; Pournasrollah, A.; Sadegh, R.; Esmaeeli, H.; Ghadimi, Y.; Razmpa, E. Quercetin Decreases Th17 Production by Down-Regulation of MAPK- TLR4 Signaling Pathway on T Cells in Dental Pulpitis. *Journal of Dentistry (Shiraz, Iran)* **2018**, *19* (4), 259−264.

(67) Zhao, X.; He, W.; Song, Z.; Tong, Z.; Li, S.; Ni, L. Mineral trioxide aggregate promotes odontoblastic differentiation via mitogen-activated protein kinase pathway in human dental pulp stem cells. *Mol. Biol. Rep.* **2012**, *39* (1), 215−220.

(68) Rong, J.; Pool, B.; Zhu, M.; Munro, J.; Cornish, J.; McCarthy, G. M.; Dalbeth, N.; Poulsen, R. Basic Calcium Phosphate Crystals Induce Osteoarthritis-Associated Changes in Phenotype Markers in Primary Human Chondrocytes by a Calcium/Calmodulin Kinase 2-Dependent Mechanism. *Calcif. Tissue Int.* **2019**, *104*, 331.

(69) Wei, Y.; Jin, Z.; Zhang, H.; Piao, S.; Lu, J.; Bai, L. The Transient Receptor Potential Channel, Vanilloid 5, Induces Chondrocyte Apoptosis via Ca^{2+} CaMKII-Dependent MAPK and Akt/ mTOR Pathways in a Rat Osteoarthritis Model. *Cell. Physiol. Biochem.* **2018**, *51* (5), 2309−2323.

(70) Dong, F.; Yang, S.; Sun, H.; Yan, J.; Guo, X.; Li, D.; Zhou, D. Persistent mechanical stretch-induced calcium overload and MAPK signal activation contributed to SCF reduction in colonic smooth muscle in vivo and in vitro AU - Dong, Fang. *J. Recept. Signal Transduction Res.* **2017**, *37* (2), 141−148.